

**Physical properties of  $(\text{Mn}_{1-x}\text{Fe}_x)\text{Si}$  at  $x \simeq 0.15$  along the critical trajectory**

A. E. Petrova

*Institute for High Pressure Physics of RAS, Troitsk, Russia*

S. Yu. Gavrilkin

*P. N. Lebedev Physical Institute, Leninsky pr., 53, 119991 Moscow, Russia*

Dirk Menzel

*Institut für Physik der Kondensierten Materie, Technische Universität Braunschweig, D-38106 Braunschweig, Germany*

S. M. Stishov\*

*Institute for High Pressure Physics of RAS, Troitsk, Moscow, Russia*

(Received 22 May 2019; revised manuscript received 17 July 2019; published 3 September 2019)

We report results of studying the magnetization, specific heat, and thermal expansion of a single crystal with nominal composition  $(\text{Mn}_{1-x}\text{Fe}_x)\text{Si}$  with  $x = 0.15$ . We found no thermodynamic evidence in favor of a second-order phase transition in this material. The trajectory corresponding to the present composition of  $(\text{MnFe})\text{Si}$  is a critical one, i.e., approaching quantum critical point at lowering temperature, but some properties may feel the cloud of helical fluctuations bordering the phase transition line.

DOI: [10.1103/PhysRevB.100.094403](https://doi.org/10.1103/PhysRevB.100.094403)**I. INTRODUCTION**

An evolution of the magnetic phase transition in the helical magnet  $\text{MnSi}$  at high pressure is reported in a number of publications [1–3]. It became clear that the phase transition temperature decreased with pressure and practically reached the zero value at  $\sim 15$  kbar. However, a nature of this transition at zero temperature and high pressure is still a subject of controversial interpretations. Early it was claimed an existence of tricritical point on the phase transition line that might result in a first-order phase transition in  $\text{MnSi}$  at low temperatures [4]. The latter would prevent an existence of quantum critical point in  $\text{MnSi}$ . This view was seemingly supported by the volume measurements at the phase transition in  $\text{MnSi}$  [5,6]. However, this idea was disputed in papers [7,8], where it was stated that the observed volume anomaly at the phase transitions in  $\text{MnSi}$  at low temperatures was simply the slightly narrowing anomaly clearly seen at elevated temperatures. On the other hand, some experimental works and the recent Monte Carlo calculations may indicate a strong influence of inhomogeneous stress arising at high pressures and low temperatures on characteristics of phase transitions that could make any experimental data not entirely conclusive [7–9].

In this situation it would be appealing to use a different approach to discover a quantum criticality in  $\text{MnSi}$ , for instance, making use doping as a controlling parameter. Indeed, it became known that doping  $\text{MnSi}$  with Fe and Co decreases a temperature of the magnetic phase transitions and finally completely suppress the transitions at some critical concentrations of the dopants. In case of Fe doping a critical concentration

consist of about  $0.15x$  (actually different estimates of  $x$  vary from 0.10 to 0.19) [10–15].

Actually, the general belief that the concentration of the dopant added to the batch will be the same in the grown crystal is incorrect. One needs to perform chemical and x-ray analyses to make a certain conclusion about the real composition of material. Anyway, there is some evidence (non-Fermi-liquid resistivity, logarithmic divergence of specific heat) that indeed the quantum critical point occurs in  $(\text{Mn}_{1-x}\text{Fe}_x)\text{Si}$  in the vicinity of iron concentration  $x = 0.15$  at ambient pressure. However, in a recent publication it is claimed that  $(\text{Mn}_{0.85}\text{Fe}_{0.15})\text{Si}$  experiences a second-order phase transition at the pressure range to  $\sim 0$ –23 kbar, therefore placing the quantum critical point in this material at high pressure [16]. To this end it seems appropriate to take another look at the situation. We report here the results of a study of a single crystal with nominal composition  $(\text{Mn}_{0.85}\text{Fe}_{0.15})\text{Si}$ . Note that we call nominal a composition that follows from proportions of ingredients initially used in a sample preparation. But a final composition may differ from a nominal one due to various factors accompanying the crystal growth.

**II. EXPERIMENT**

The sample  $(\text{MnFe})\text{Si}$  was prepared from the ingot obtained by premelting of Mn (purity 99.99%; Chempur), Fe (purity 99.98%; Alfa Aesar), and Si ( $\rho_n = 300 \Omega \text{ cm}$ ,  $\rho_p = 3000 \Omega \text{ cm}$ ) under argon atmosphere in a single arc oven, then a single crystal was grown using the triarc Czochralski technique. The electron-probe microanalysis shows that real composition is  $(\text{Mn}_{0.74}\text{Fe}_{0.15})\text{Si}$ , which indicates some deviations from the stoichiometric chemical compositions common to the silicide compounds. The independent Rietveld analysis

\*sergei@hppi.troitsk.ru

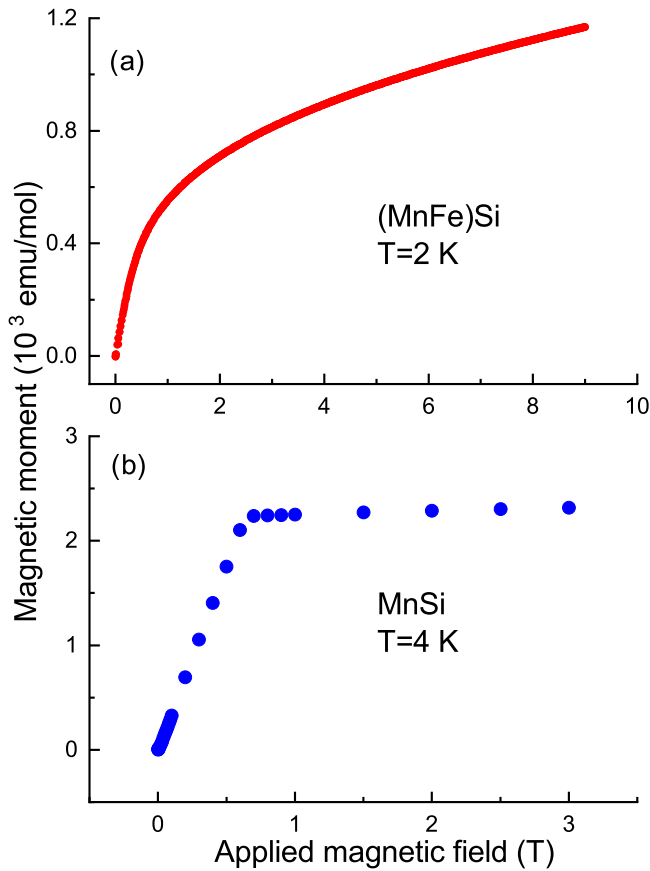


FIG. 1. Magnetization curves for (MnFe)Si (a) and MnSi (b) [7,18].

also showed that  $x \sim 0.15$ . Hereafter we will call the sample under study (MnFe)Si.

The lattice parameter of the sample appeared to be  $a = 4.5462 \text{ \AA}$ . Note that the lattice parameter of pure MnSi is somewhat higher and equal to  $a = 4.5598 \text{ \AA}$ . This implies that iron plays a role of some sort of pressure agent.

We performed some magnetic, dilatometric, electrical, and heat capacity measurements to characterize the sample of (MnFe)Si. All measurements were made making use of a Quantum Design PPMS system with the heat capacity and vibrating magnetometer moduli and the He-3 Refrigerator. The linear expansion of the sample was measured by the capacity dilatometer [17]. The resistivity data were obtained with the standard four-terminal scheme using spark welded Pt wires as electrical contacts. The sample resistance was measured in a (100) plane. Magnetic field, when applied, was always directed along [100].

The experimental results are displayed in Figs. 1–11. Whenever it is possible the corresponding data for pure MnSi are depicted at the same figures to facilitate comparisons of the data.

In Fig. 1 the magnetization curves for both (MnFe)Si and MnSi are shown. As follows, the magnetization of (MnFe)Si (a) does not reveal an existence of the spontaneous magnetic moment in contrast with a case of MnSi. From the saturated magnetization of MnSi at high field [Fig. 1(b)], the magnetic moment per atom Mn is  $0.4\mu_B$ .

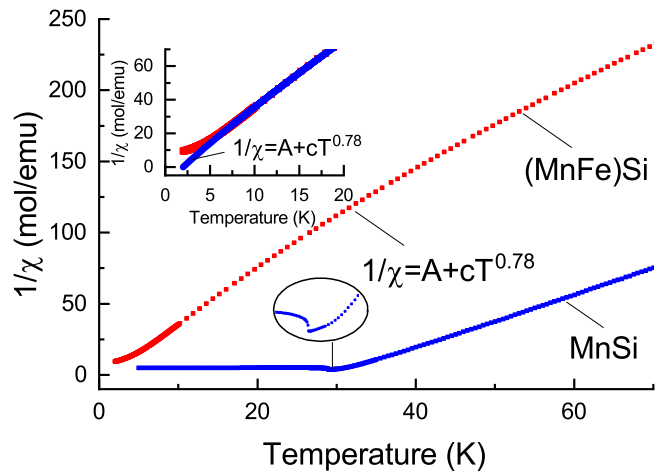


FIG. 2. The inverse magnetic susceptibility  $1/\chi$  for (MnFe)Si and MnSi [7,18] as measured at 0.01 T.

As seen from Fig. 2 the magnetic susceptibility  $\chi$  of (MnFe)Si does not obey the Curie-Weiss law, which clearly works in the paramagnetic phase of MnSi. The temperature dependence of  $1/\chi$  for (MnFe)Si is well described in the range 5–150 K by the expression  $1/\chi = A + cT^{0.78}$ , which was also observed for some substances with quantum critical behavior [22]. This expression can be rewritten in the form  $(1/\chi - 1/\chi_0)^{-1} = cT^{-1}$ , implying a divergence of the quantity  $(1/\chi - 1/\chi_0)^{-1}$ . The nature of the anomalous part of the  $1/\chi$  at  $< 5 \text{ K}$  (see inset in Fig. 2) will be discussed later.

As can be seen from Fig. 3, magnetic field does not much influence the specific heat of (MnFe)Si at least at high temperatures. Also seen in the inset of Fig. 3 is that the ratio of  $C_p/T$  does not well fit the logarithmic law.

The power-law behavior of  $C_p$  in the range 0.4–4 K is characterized by the exponent  $\sim 0.77$  (Fig. 4), which immediately leads to the diverging expression for  $C_p/T \sim T^{-1+0.77}$  [see Fig. 5(b)]. This finding contradicts the data [12] declaring the

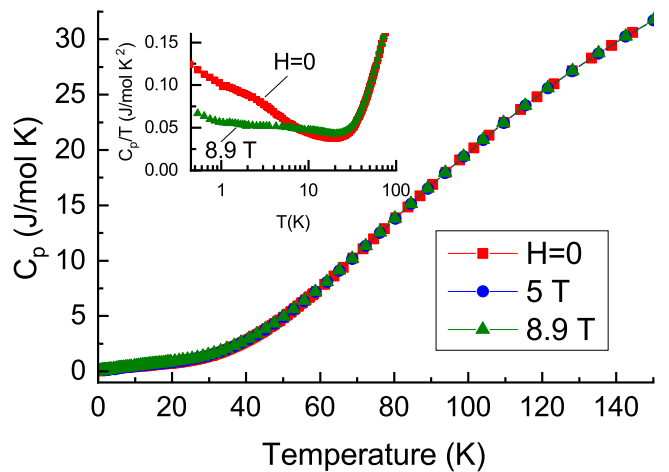


FIG. 3. Specific heat of (MnFe)Si as a function of temperature at different magnetic fields. Specific heat of (MnFe)Si divided by temperature  $C_p/T$  is shown in the inset in logarithmic scale at zero magnetic field.

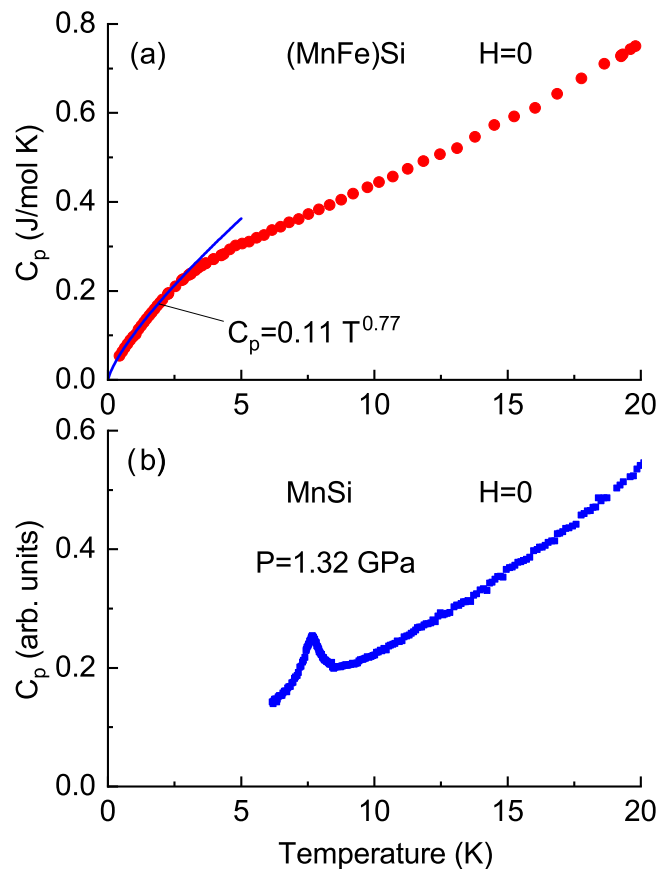


FIG. 4. (a) Specific heat of  $(\text{MnFe})\text{Si}$  as a function of temperature in the 0.4–20 K range. The line is the power function fit to the experimental data (shown in the plot). (b) Specific heat of  $\text{MnSi}$  at high pressure measured by the ac calorimetry technique [19].

logarithmic divergence of  $C_p/T$  for  $(\text{MnFe})\text{Si}$  in about the same temperature range (see the inset in Fig. 3). In Fig. 4(b) is shown how the phase transition in  $\text{MnSi}$  at high pressure close to the quantum critical region influences the specific heat. An additional illustration of this kind is provided by the resistivity data (see Fig. 11). So one cannot find any similar evidence in Fig. 4(a) for the would-be phase transition, which was suggested in Ref. [16].

Figure 5 shows the temperature dependences of specific heats  $C_p$  (a) and specific heats divided by temperature  $C_p/T$  (b) for  $(\text{MnFe})\text{Si}$  and  $\text{MnSi}$ . As can be seen, both quantities do not differ much at temperatures above the magnetic phase transitions in  $\text{MnSi}$  even with applied magnetic field. The great difference arises at and below phase transition temperatures in  $\text{MnSi}$ . The remarkable thing is the diverging behavior of  $C_p/T$  that is suppressed by an application of strong magnetic field [Fig. 5(b)] though the divergence of  $C_p/T$  still exists at low temperatures ( $<1$  K).

As seen in Fig. 6, the magnetic phase transition in  $\text{MnSi}$  is signified by a significant volume anomaly. Nothing of this kind exists on the thermal expansion curve of  $(\text{MnFe})\text{Si}$ . Probably a somewhat different situation can be observed in Fig. 7, which displays the temperature dependences of linear thermal expansion coefficients  $\beta = (1/L_0)(dL/dT)_p$  for  $(\text{MnFe})\text{Si}$  and  $\text{MnSi}$ . A surprisingly good agreement is seen

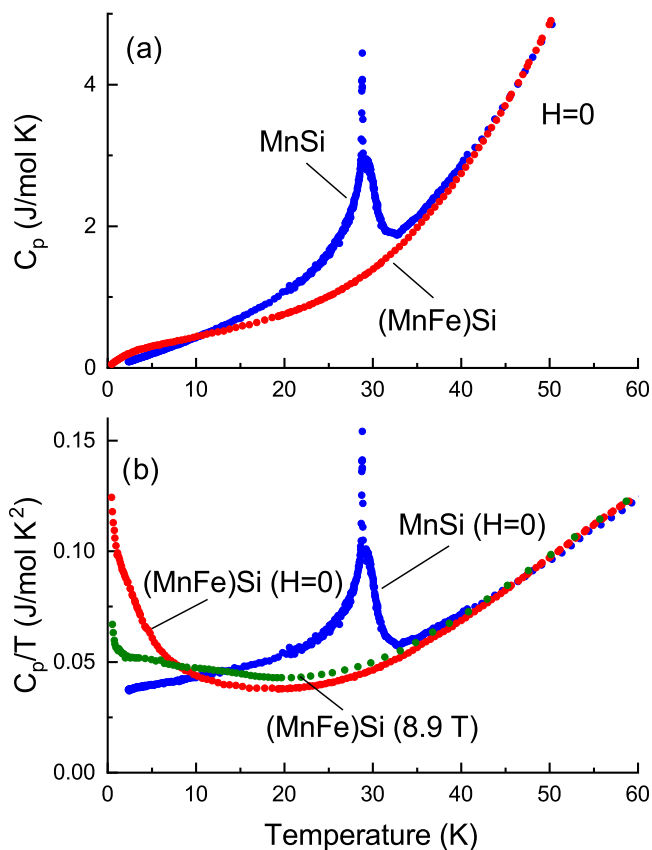


FIG. 5. Temperature dependence of  $C_p$  (a) and  $C_p/T$  (b) for  $(\text{MnFe})\text{Si}$  and  $\text{MnSi}$  [7,20].

between both data at high temperature. A specific feature of  $\beta$  of  $(\text{MnFe})\text{Si}$  is a small tail at  $T < 5$  K. This tail is inclined to cross the temperature axis at finite value, therefore tending to the negative  $\beta$  as it does occur in  $\text{MnSi}$  in the phase transition region (see Figs. 7 and 8). Just this behavior of  $\beta$  creates a sudden drop at low temperatures in the seemingly diverging ratio  $\beta/C_p$ , which conditionally may be called the Gruneisen parameter,  $\Gamma$  (see Fig. 9). Note that the divergent  $\Gamma$  implies

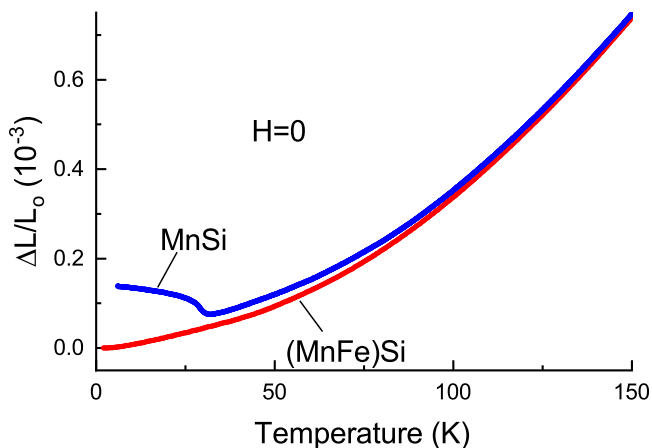


FIG. 6. Dependence of linear thermal expansion of  $(\text{MnFe})\text{Si}$  and  $\text{MnSi}$  [7,20] on temperature.  $\text{MnSi}$  data reduced to that of  $(\text{MnFe})\text{Si}$  at 200 K for better viewing.

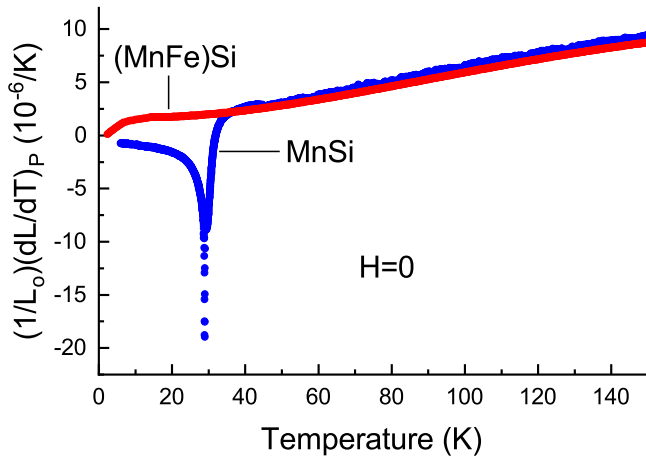


FIG. 7. Linear thermal expansion coefficients of (MnFe)Si and MnSi [7,20].

vanishing some energy scale which is expected at the quantum critical point (see Ref. [23]).

Figure 8 shows that magnetic field strongly influences the “tail” region of the thermal expansion coefficient of (MnFe)Si that indicates its fluctuation nature. This feature should be linked to the anomalous part of the  $1/\chi$  at  $<5$  K (Fig. 2).

Resistivities of (MnFe)Si and MnSi as functions of temperature are shown in Fig. 10. The quasilinear non-Fermi-liquid behavior of resistivity of (MnFe)Si at low temperature in contrast with the MnSi case is quite obvious. With increasing temperature the resistivity of (MnFe)Si evolves to the “saturation” curve typical of the strongly disordered metals and similar to the post phase transition branch of the resistivity curve of MnSi [24].

A comparison of Figs. 11(a) and 11(b) shows a drastic difference in behavior of  $d\rho/dT$  at the phase transition in MnSi and in (MnFe)Si in the supposedly critical region. The peculiar form of  $d\rho/dT$  of (MnFe)Si does not look like a phase transition feature although it certainly reflects an existence of significant spin fluctuations. This feature should be related to the anomalies of the magnetic susceptibility (Fig. 2) and thermal expansion coefficient (Fig. 8).

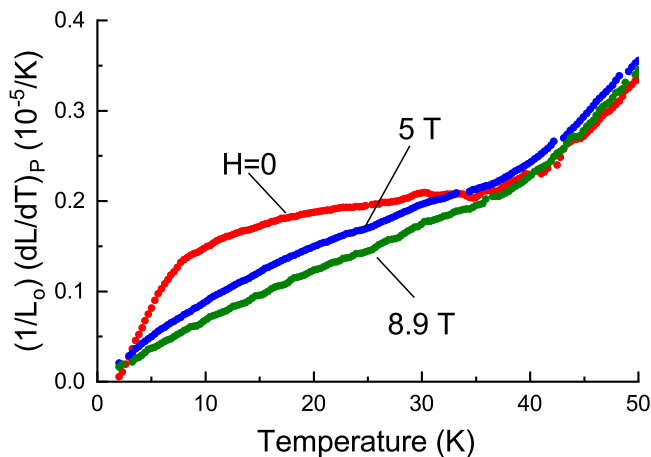


FIG. 8. Linear thermal expansion coefficients of (MnFe)Si as functions of temperature and magnetic fields.

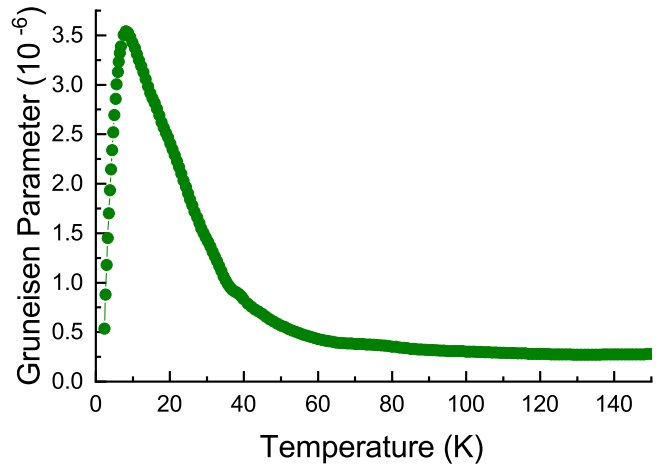


FIG. 9. Gruneisen ratio tends to diverge at  $T \rightarrow 0$ . This tendency is interrupted by a peculiar behavior of the thermal expansion coefficient.

### III. DISCUSSION

As we have shown earlier, the lattice parameter of our sample of (MnFe)Si is somewhat less than that of pure MnSi at ambient pressure. Let us estimate what pressure is needed to compress pure MnSi to the volume corresponding to the lattice parameter of the material under study. We use a simple linear expression of the form  $P = K \frac{\Delta V}{V}$ , where  $P$  is pressure,  $K = -V(\frac{dP}{dV})_T$  is bulk modulus, and  $\frac{\Delta V}{V} = (V_{\text{MnSi}} - V_{(\text{MnFe)Si}})/V_{(\text{MnFe)Si}}$ . Taking  $K = 1.64$  Mbar [25] and  $\frac{\Delta V}{V} = 8.96 \times 10^{-3}$  (it follows from the lattice parameter values given above), one obtains  $P = 14.63$  kbar. Surprisingly this value practically coincides with the pressure corresponding to the phase transition in the pure MnSi at zero temperature [1–4]. At this pressure and zero temperature the quantum phase transition in MnSi does occur, the nature and properties of which are still under discussion [7]. With the above argument in favor of quantum criticality of (MnFe)Si in the vicinity of iron concentration  $x = 0.15$ , an alternative way to reach the quantum regime is to use so-called

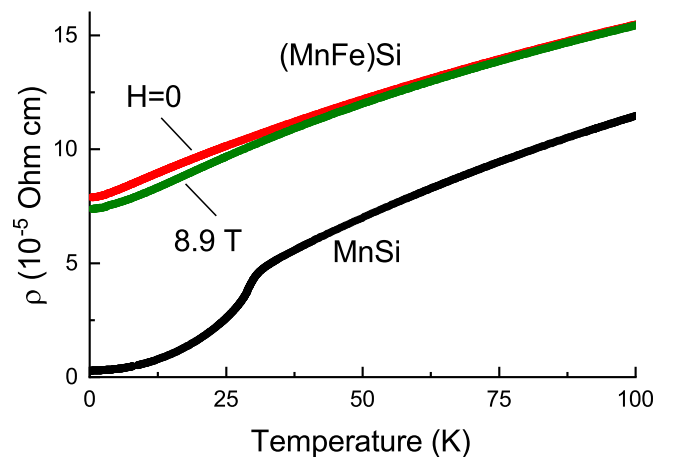


FIG. 10. Resistivities of (MnFe)Si and MnSi [21] as functions of temperature.

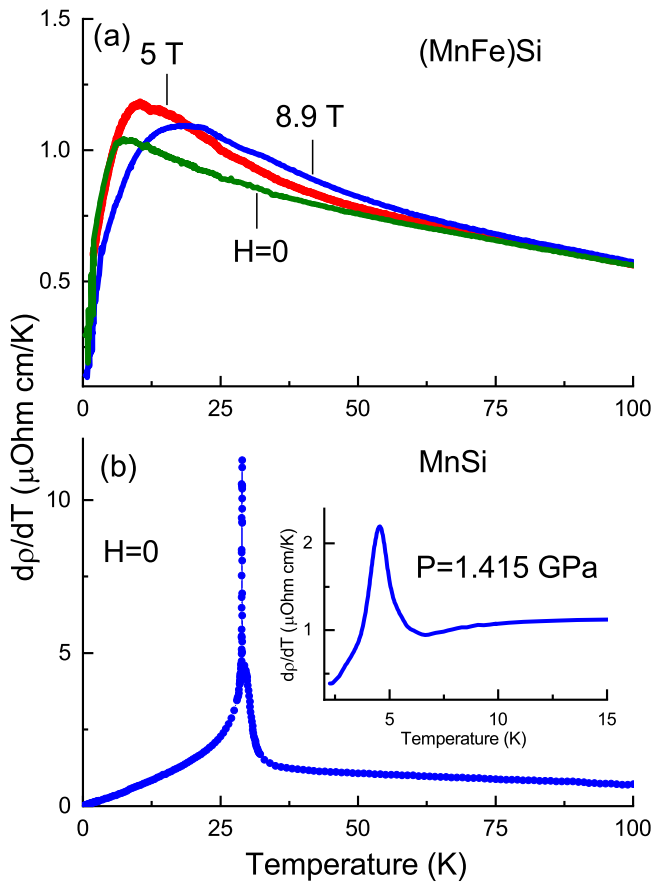


FIG. 11. Dependence of temperature derivative of resistivity of  $(\text{MnFe})\text{Si}$  and  $\text{MnSi}$  on temperature: (a)  $d\rho/dT$  of  $(\text{MnFe})\text{Si}$  as functions of temperature and magnetic fields; (b)  $d\rho/dT$  of  $\text{MnSi}$  as a function of temperature at ambient and high pressure (in the inset) [8,21].

“chemical pressure” doping  $\text{MnSi}$  with suitable “dopants.” That could avoid disturbing inhomogeneous stresses arising at conventional pressure loading. So as it appears, the composition  $\text{Mn}_{0.85}\text{Fe}_{0.15}\text{Si}$  indeed demonstrated properties typical of the quantum critical state [11,12]. However, the conclusions of Refs. [11,12] were disputed in the publication [16], the authors of which claim on the basis of the muon spin relaxation experiments that  $(\text{Mn}_{1-x}\text{Fe}_x)\text{Si}$  at  $x \simeq 0.15$  experiences a second-order phase transition at ambient pressure, then reaching a quantum critical point at pressure  $\sim 21\text{--}23$  kbar.

With all that in mind we have carried out a number of measurements trying to elucidate the problem. Below we summarize our findings.

(1) There is no spontaneous magnetic moment in  $(\text{MnFe})\text{Si}$ , at least at 2 K (Fig. 1). Magnetic susceptibility of  $(\text{MnFe})\text{Si}$  can be described by the expression  $1/\chi = A + cT^{0.78}$  or  $(1/\chi - 1/\chi_0)^{-1} = cT^{-1}$  in the temperature range  $\sim 5 - 150$  K, implying divergence of the quantity  $(1/\chi - 1/\chi_0)^{-1}$ . This behavior also was observed earlier in the case of some substances close to quantum critical region (Fig. 2) [22]. At  $T < 5$  K a behavior of  $1/\chi$  deviates from the mentioned expression in a way, which can be traced to the analogous

feature at the fluctuation region of  $\text{MnSi}$  at  $T > T_c$  (see the round inset in Fig. 2).

(2)  $C \sim T^{0.77}$  in the range 2–20 K, which does not show any features inherited to phase transitions as takes place in the case of  $\text{MnSi}$  at pressure close to the quantum phase transition (Figs. 3 and 4). This expression immediately leads to the divergence of the quantity  $C_p/T \sim T^{-1+0.77}$ , which can be suppressed by a magnetic field that leads to restoring the Fermi-liquid picture with finite value of electronic specific heat term  $\gamma$  (Fig. 5).

(3) The thermal expansion experiment with  $(\text{MnFe})\text{Si}$  does not reveal any features that can be linked to a phase transition (Fig. 6). However, the thermal expansion coefficient  $\beta$  shows a low-temperature tail, which inclines to cross the temperature axis at finite value tending to become negative as it occurs in  $\text{MnSi}$  (Figs. 7 and 8). This specifics of  $\beta$  causes a sudden low-temperature drop of the Gruneisen parameter, otherwise it would diverge at  $T \rightarrow 0$ . An application of magnetic field suppresses this kind of behavior of the thermal expansion coefficient, therefore revealing its fluctuation nature (Fig. 8).

(4) The resistivity of  $(\text{MnFe})\text{Si}$  clearly demonstrates non-Fermi-liquid behavior with no specifics indicating a phase transition. However, the temperature derivative of resistivity  $d\rho/dT$  of  $(\text{MnFe})\text{Si}$  shows nontrivial form, which indicates an existence of significant spin fluctuations. That should be related with the low-temperature tails both magnetic susceptibility and thermal expansion coefficient.

#### IV. CONCLUSION

Finally, magnetic susceptibility in the form  $(1/\chi - 1/\chi_0)^{-1}$  and Gruneisen parameter  $\beta/C_p$  in  $(\text{MnFe})\text{Si}$  show diverging behavior, which is interrupted at about 5 K by factors linked somehow with spin fluctuation analogs to ones preceding the phase transition in  $\text{MnSi}$  (see Figs. 2, 7, and 8). The specific heat divided by temperature  $C_p/T$  of  $(\text{MnFe})\text{Si}$  clearly demonstrates diverging behavior to 2 K. The electrical resistivity of  $(\text{MnFe})\text{Si}$  exhibits non-Fermi-liquid character.

Our general conclusions are as follows: There are no thermodynamic evidences in favor of a second-order phase transition for the  $(\text{Mn}_{1-x}\text{Fe}_x)\text{Si}$  at  $x \simeq 0.15$ . The trajectory corresponding to the present composition of  $(\text{MnFe})\text{Si}$  is a critical one, i.e., approaching quantum critical point at lowering temperature, which agrees with the conclusions made in Refs. [11,12]. However, the critical trajectory in fact is a tangent to the phase transition line and therefore some properties inevitably would be influenced by the cloud of spin helical fluctuations bordering the phase transition (see Ref. [14]). This situation produces some sort of a mixed state instead of a pure quantum critical one that probably was seen in the experiments [16].

#### ACKNOWLEDGMENTS

We express our gratitude to I. P. Zibrov and N. F. Borovikov for technical assistance. A.E.P. and S.M.S. greatly appreciate the financial support of the Russian Foundation for Basic Research (Grant No. 18-02-00183) and the Russian Science Foundation (Grant No. 17-12-01050).

- [1] J. D. Thompson, Z. Fisk, and G. G. Lonzarich, *Phys. B (Amsterdam, Neth.)* **161**, 317 (1989).
- [2] C. Pfleiderer, G. J. McMullan, and G. G. Lonzarich, *Phys. B (Amsterdam, Neth.)* **206–207**, 847 (1995).
- [3] C. Thessieu, J. Flouquet, G. Lapertot, A. N. Stepanov, and D. Jaccard, *Solid State Commun.* **95**, 707 (1995).
- [4] C. Pfleiderer, G. J. McMullan, S. R. Julian, and G. G. Lonzarich, *Phys. Rev. B* **55**, 8330 (1997).
- [5] C. Pfleiderer, P. Böni, T. Keller, U. K. Rößler, and A. Rosch, *Science* **316**, 1871 (2007).
- [6] A. Miyake, A. Villaume, Y. Haga, G. Knebel, B. Salce, G. Lapertot, and J. Flouquet, *J. Phys. Soc. Jpn.* **78**, 044703 (2009).
- [7] S. M. Stishov and A. E. Petrova, *Phys. Usp.* **54**, 1117 (2011).
- [8] A. E. Petrova and S. M. Stishov, *Phys. Rev. B* **86**, 174407 (2012).
- [9] A. M. Belemuk and S. M. Stishov, *J. Phys.: Condens. Matter* **31**, 135801 (2019).
- [10] S. V. Grigoriev, V. A. Dyadkin, E. V. Moskvina, D. Lamago, Th. Wolf, H. Eckerlebe, and S. V. Maleyev, *Phys. Rev. B* **79**, 144417 (2009).
- [11] *Properties and Applications of Thermoelectric Materials*, 261 *NATO Science for Peace and Security Series B: Physics and Biophysics*, edited by C. Meingast, Q. Zhang, T. Wolf, F. Hardy, K. Grube, W. Knafo, P. Adelman, P. Schweiss, H. v. Löhneysen, V. Zlatić, and A. C. Hewson (Springer Science-Business Media B. V., Berlin, 2009).
- [12] A. Bauer, A. Neubauer, C. Franz, W. Münzer, M. Garst, and C. Pfleiderer, *Phys. Rev. B* **82**, 064404 (2010).
- [13] J. Kindervater, T. Adams, A. Bauer, F. Haslbeck, A. Chacon, S. Mühlbauer, F. Jonietz, A. Neubauer, U. Gasser, G. Nagy, N. Martin, W. Häußler, R. Georgii, M. Garst, and C. Pfleiderer, [arXiv:1811.12379v1](https://arxiv.org/abs/1811.12379v1).
- [14] L. J. Bannenberg, R. M. Dalgliesh, T. Wolf, F. Weber, and C. Pappas, *Phys. Rev. B* **98**, 184431 (2018).
- [15] L. J. Bannenberg, F. Weber, A. J. E. Lefering, T. Wolf, and C. Pappas, *Phys. Rev. B* **98**, 184430 (2018).
- [16] T. Goko, C. J. Arguello, A. Hamann, T. Wolf, M. Lee, D. Reznik, A. Maisuradze, R. Khasanov, E. Morenzoni, and Y. J. Uemura, *npj Quantum Mater.* **2**, 44 (2017).
- [17] M. Rotter, H. Müller, E. Gratz, M. Doerr, and M. Loewenhaupt, *Rev. Sci. Instrum.* **69**, 2742 (1998).
- [18] S. M. Stishov, A. E. Petrova, S. Khasanov, G. Kh. Panova, A. A. Shikov, J. C. Lashley, D. Wu, and T. A. Lograsso, *Phys. Rev. B* **76**, 052405 (2007).
- [19] V. A. Sidorov, A. E. Petrova, P. S. Berdonosov, V. A. Dolgikh, and S. M. Stishov, *Phys. Rev. B* **89**, 100403(R) (2014).
- [20] S. M. Stishov, A. E. Petrova, S. Khasanov, G. Kh. Panova, A. A. Shikov, J. C. Lashley, D. Wu, and T. A. Lograsso, *J. Phys.: Condens. Matter* **20**, 235222 (2008).
- [21] A. E. Petrova, E. D. Bauer, V. Krasnorussky, and S. M. Stishov, *Phys. Rev. B* **74**, 092401 (2006).
- [22] P. Coleman, *Phys. B (Amsterdam, Neth.)* **259–261**, 353 (1999).
- [23] L. Zhu, M. Garst, A. Rosch, and Q. Si, *Phys. Rev. Lett.* **91**, 066404 (2003).
- [24] H. Wiesmann, M. Gurvitch, H. Lutz, A. Ghosh, B. Schwarz, M. Strongin, P. B. Allen, and J. W. Halley, *Phys. Rev. Lett.* **38**, 782 (1977).
- [25] A. E. Petrova and S. M. Stishov, *J. Phys.: Condens. Matter* **21**, 196001 (2009).